Available online at www.sciencedirect.com
SCIENCE DIRECT®

Journal of the European Ceramic Society 24 (2004) 271–276

www.elsevier.com/locate/jeurceramsoc

(Ba,Sr)TiO_3 thin film growth in a batch processing MOCVD reactor

S. Regnery[a,b,*], P. Ehrhart[a], F. Fitsilis[a], R. Waser[a], Y. Ding[c], C.L. Jia[c], M. Schumacher[b], F. Schienle[b], H. Juergensen[b]

[a] *IFF/EKM-Forschungszentrum Jülich, Germany*
[b] *Aixtron AG Aachen, Germany*
[c] *IFF/MSF-Forschungszentrum Jülich, Germany*

Abstract

Thin films of different compositions within the (Ba_x,Sr_{1-x})TiO_3 solid solution series were deposited in a planetary multi-wafer MOCVD reactor using different solutions of $Sr(thd)_2$, $Ba(thd)_2$ and $Ti(O\text{-}i\text{-}Pr)_2(thd)_2$ precursors. Structural and electrical properties of Pt/BST/Pt MIM structures are presented. On the base of film thickness series ranging from 10 to 150 nm the electrical permittivity is discussed within the dead layer model. The performance of two different liquid precursor delivery systems, characterized by flash evaporation and liquid injection, respectively, are compared for the example of different $SrTiO_3$ films. Finally, the growth of $SrTiO_3$ on Pt(111) is compared with the growth on Si(100) and the electrical characteristics of the Pt/STO/Si MIS structures are discussed.

Keywords: $BaTiO_3$ and titanates; Capacitors; Dielectric properties; Electron microscopy; Thin films

1. Introduction

High dielectric constant perovskite thin films, such as the $Ba_xSr_{1-x}TiO_3$, (BST), solid solution series have been proposed for a very broad application area, including capacitor dielectrics for future dynamic random access memories (DRAMs), embedded capacitors, tunable devices, as well as gate oxides for field effect transistors (FETs).[1] For capacitor applications, i.e. metal-insulator-metal (MIM) structures, there is a wide experience on the growth on suitable electrodes, and Pt might be considered as a standard metal. For gate-oxide applications metal-insulator-semiconductor (MIS) structures must be deposited. An ultra thin oxide layer should be grown directly on Si without interfacial SiO_x layers, which reduce the capacitance of the layer stack.[2] Amorphous metal oxides, like Al_2O_3, HfO_2, and ZrO_2, with *K*-values in the range of 8–20, are considered as the most promising near term replacement of the presently used SiO_2. For even higher *K*-values crystalline materials, especially $SrTiO_3$ (STO), are considered as epitaxial layers and, in spite of the possible complications by grain boundaries, also in the form of polycrystalline films.

In order to optimize the growth conditions for the different applications of these films we investigated the metal organic chemical vapor deposition (MOCVD) of thin BST films of different composition and on different substrates. We first report on the growth of (Ba,Sr)TiO_3 on Pt(111) and the electrical properties of the resulting MIM structures. Secondly we compare STO films deposited with different evaporation systems and finally we compare the growth of STO on Pt(111) and Si(100) substrates.

2. Experimental

2.1. Film deposition

Films were deposited in a Aixtron 2600G3 Planetary Reactor®, which can handle five 6-inch wafer simultaneously. This reactor is characterized by a central gas inlet providing a pure horizontal gas flow, which makes this reactor a radial flow system.[3] The process conditions are summarized in Table 1. The deposition temperature is characterized by the suszeptor temperature, however, the actual wafer surface temperature may deviate by several degrees and depends on the details of the process and on the wafer surface, for example, platinized wafers have somewhat higher temperatures than oxidized wafers. The film composition was routinely determined by XRF and film thickness growth rates and precursor incorporation efficiencies were deduced from these data.

* Corresponding author.
E-mail address: s.regnery@fz-juelich.de (S. Regnery).

0955-2219/03/$ - see front matter © 2003 Elsevier Ltd. All rights reserved.
doi:10.1016/S0955-2219(03)00235-8

Table 1
Growth conditions

Susceptor temperature	650 °C	
Reactor pressure	1–2 mbar	
Film thickness	10–150 nm	
	ATMI-300B	TRIJET®
Vaporization temperature	240 °C	240 °C
Growth rate [nm/min]	2.7	11.3
Liquid source feeding rate	0.08 ml/min (typically 0.35 molar)	1.9 ml/min (typically 0.05 molar)

Two vaporizer systems were compared. In the first case we used a liquid delivery system, ATMI-300B which mixes the liquid precursors of up to four different sources, in our case 0.35 molar solutions of $Sr(thd)_2$, $Ba(thd)_2$ and a 0.4 molar solution of $Ti(O\text{-}iPr)_2(thd)_2$. The liquid mixture is delivered by a micro-pump to the vaporizer, which is basically a sintered metal frit heated at 240 °C. Once in contact with the frit the precursor evaporates abruptly. In order to avoid clogging of the frit the evaporation rate is limited to about 0.08 ml/s which limits also the growth rate for our 5×6 inch reactor.

In the second case we use a TRIJET® vaporizer. Due to the non-contact evaporation clogging is prevented and rather high evaporation rates can be achieved. Four independent inject valves directly feed into the vaporization chamber. For deposition of STO we used the same precursors as in the previous case, but for reliable processing a higher dilution is recommended and a 0.05 molar solution was used. The amount of precursor delivery depends on the source pressure (1100 mbar), the opening time of the inject valves (0.8 ms) and the frequency of injection pulses. After optimizing the deposition process and especially the homogeneity on the 6 inch wafers we used 6.25 pulses per second, which is 3.125 pulses per second of each of the two sources used for STO. The main advantage for our applications are the separate injection valves which allow for a variability concerning source selection and concentration during film growth.

2.2. Electrical properties

For the electrical characterization Pt top electrodes were deposited by magnetron sputtering. Electrode size of a diameter between 0.1 and 1.13 mm were obtained by lift-off process. For the Pt/BST/Pt MIM structures an additional post-annealing process was performed, generally at 550 °C for 20 min in oxygen. For the Pt/BST/Si MIS structures grown on *p*-type Si(100) an eutectic Ga–In alloy was used to form an ohmic contact to the Si backside electrode. The C–V characteristics were measured with a HP4284A LCR meter. For the MIM structures a standard frequency of 1 kHz was used whereas 100kHz were applied for the MIS structures in order to reach the HF characteristics.

It is generally observed that the permittivity of high-K thin films capacitors shows some thickness dependence, which can be phenomenological described by an interfacial layer. This model assumes a bulk region of thickness, t, and the two interface regions adjacent to the electrodes with thickness, t_i, which yield two capacitors of a lower permittivity. Considering the two electrodes as identical the resulting reciprocal capacitance of the film is given by Eq. (1). By further approximating $(t-2t_i)$ by t, the slope of a plot of 1/C versus thickness reveals the bulk permittivity, while the intercept represents the interface capacitance, $2A/C_i$ or the value of $2t_i/\varepsilon_0\varepsilon_i$.

$$\frac{A}{C} = \frac{2 \times A}{C_i} + \frac{A}{C_B} = \frac{2 \times t_i}{\varepsilon_0 \times \varepsilon_i} + \frac{t - 2t}{\varepsilon_0 \times \varepsilon_B} \quad (1)$$

In the following we will consider the values of ε_i/t_i, which represent an average of the two interfaces.

3. Experimental results

3.1. BST on Pt(111)

The growth behavior of $(Ba_{0.7}Sr_{0.3})TiO_3$, short BST(70/30), had been investigated in detail previously[4] and we concentrate here on depositions at a temperature of 655 °C. These films were generally characterized by a nearly perfect (100)-texture and Fig. 1 summarizes the changes of the XRD diagrams with changing (Ba/Sr) ratio. All films were grown at 655 °C with a thickness between 23 and 26 nm. The composition was slightly GrII rich (GrII/Ti = 1.01–1.05) and the (Ba/Sr) ratio was varied from 70/30 to 0/100 (pure STO) as indicated in the figure. With decreasing Ba content we observe the expected shift of the (h00) peaks, and the decrease of the height of the (100) superstructure reflection as compared to the (200) fundamental reflection. For low Ba content there is in addition some indication of the (110) reflection; these deviations from the perfect (100)-texture indicate a less stable growth. TEM micrographs, Fig. 2, show in addition, that for pure STO these different film orientations are formed both in the nucleation phase (Fig. 2a), as well as during further film growth (Fig. 2b). Due to this disruption of the columnar growth there is a trend for a more random texture for thicker films. However, there is no transition to a (111)-texture which might be expected due to the perfect lattice match in this stoichiometry region and which has been observed for CSD grown $SrTiO_3$ films.[5] The effective permittivity of these films decreases from values of 200–240 for BST(70/30) to values of 120–150 for pure STO. No significant dependency on variations of the texture of the STO films was revealed.

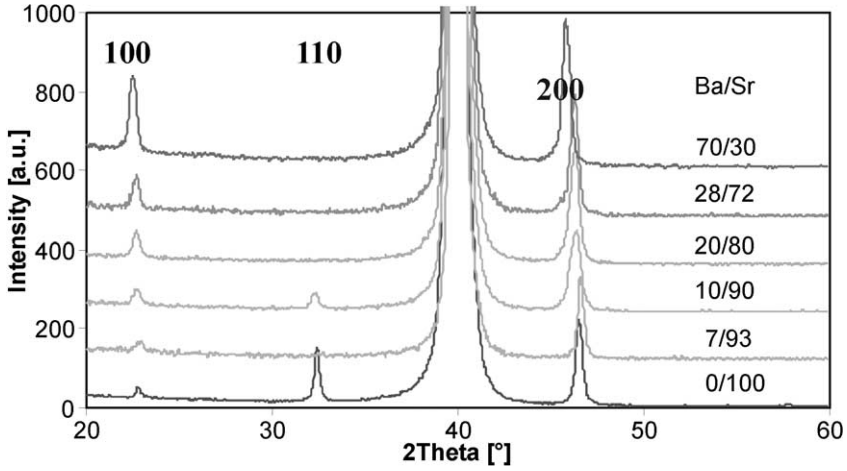

Fig. 1. XRD-diagrams of BST films with thickness of ≈30 nm deposited at 655 °C. Films are shown with decreasing Ba content as indicated in the figure.

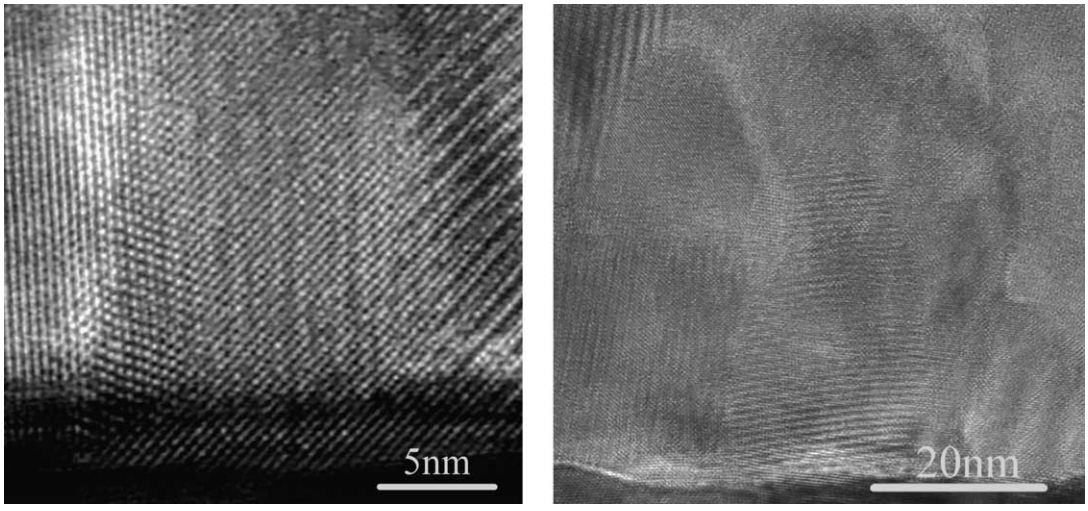

Fig. 2. Cross-sectional HRTEM images of the STO/Pt films: (a) nucleation of different grain orientations at the Pt/STO interface. (b) Occasional disruption of the columnar growth in STO films.

3.2. STO deposition on Pt(111) with different vaporizers

In order to allow a detailed discussion of the electrical film properties thickness series are necessary in order to separate effects of the interface and the bulk. Therefore several STO thickness series were performed. Fig. 3a compares the reciprocal capacity of two series for slightly Gr-II rich films as obtained for optimized conditions with the different vaporizers (Table 1). Fig. 3b shows the results for Ti-rich films as compared to the Gr-II rich films both obtained with the TRIJET®. Again no significant difference could be observed. The quantitative results are summarized in Table 2 and are discussed later.

Additional thickness series were performed with the TRIJET® vaporizer in order to test changes of the

Table 2
Results of different thickness series

Substrate	Film	Vaporizer	GrII/Ti range	ε (bulk)	ε_i/t_i (nm^{-1})
Pt(111)	BST 70/30	ATMI-300B	1.03–1.10	450±20	28±6
		ATMI-300B	0.91–0.95	837±10	14±4
	STO	ATMI-300B	1.01–1.05	208±10	41±6
		TRIJET®	1.01–1.05	215±10	26±5
		TRIJET®	0.92–0.99	208±10	34±6
Si(100)	STO	ATMI-300B	0.88–1.12	200±100	0.9[a]

[a] For this value it is assumed that the main influence of the interface results from the transition between silicon and STO, hence the influence to the platinum interface was neglected.

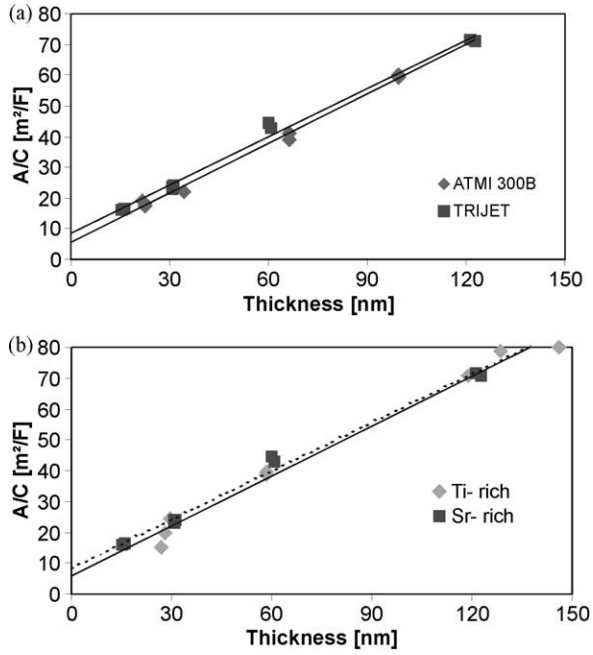

Fig. 3. Reciprocal capacitance for different STO thickness series. (a) Sr-rich films deposited with the ATMI-300B and the TRIJET® respectively. (b) Comparison of Ti-rich films to Sr-rich films (data of part a) both deposited with the TRIJET® vaporizer.

growth sequence: (a) the sequence was changed from a simultaneous deposition to alternating growth of each element: the deposition time for a monolayer was estimated from the average growth rates and monolayers of strontiumoxide or titaniumoxide were deposited with an interrupt of 5 s between the activation of the different sources. (b) Deposition of a Sr-rich interfacial layer: an interface layer (Sr/Ti = 1.2) of a thickness of 2 nm at the electrodes, and a bulk stoichiometry of Sr/Ti = 0.98. This profile was qualitatively established by STEM with a Philips CM20-FEG electron microscope. However, both variations did not result in a significant change of the electrical properties of the STO films.

3.3. STO on Si(100)

Independent of the pretreatment, i.e. a native oxide layer or a HF-dip before deposition, an oxide layer of 2–3 nm thickness is observed between the *p*-type Si and the STO, Fig. 4 (for details see Ref. 6). The grain size of these STO films is smaller and more randomly distributed than for depositions on Pt. XRD peaks are much better resolved in a thin film geometry and Fig. 5 shows as an example a 20 nm thick STO film measured with an incident angle of 2°. The differences in peak width and texture become obvious from a comparison to the sharp peaks in Fig. 1.

The planetary reactor in principle allows the deposition on both substrates simultaneously. In case of the ATMI vaporizer the strontium efficiency was slightly increased compared with depositions on platinum (7%) whereas the Ti efficiency was slightly decreased (1%). Hence, the resulting films were slightly more Sr-rich than the films deposited on Pt. For the Trijet® vaporizer major differences were observed: the strontium efficiency showed the same tendency (2.5%) but the Ti efficiency was about 31% reduced on Silicon substrates. This different behavior of the two vaporizers is not yet understood and might be due to the increased solvent concentration or the higher growth rate in combination with possible catalytic effects in the case of the Pt interface.

A typical C–V curve for the Pt/STO/SiO_x/*p*-Si/(Ga–In) MIS structure is shown in Fig. 6. For the following discussion we extracted the capacitance in the accumulation region for a comparison to the MIM structures, Table 2. Fig. 7 summarizes the capacity data for several films in a 1/C plot. As compared to Fig. 3 we observe a small interfacial capacity, which in this case corresponds to the SiO_x layer (Fig. 4) and, in spite of the large uncertainty due to the limited thickness range, the slope yields a similar bulk value for the STO film as for the MIM structures.

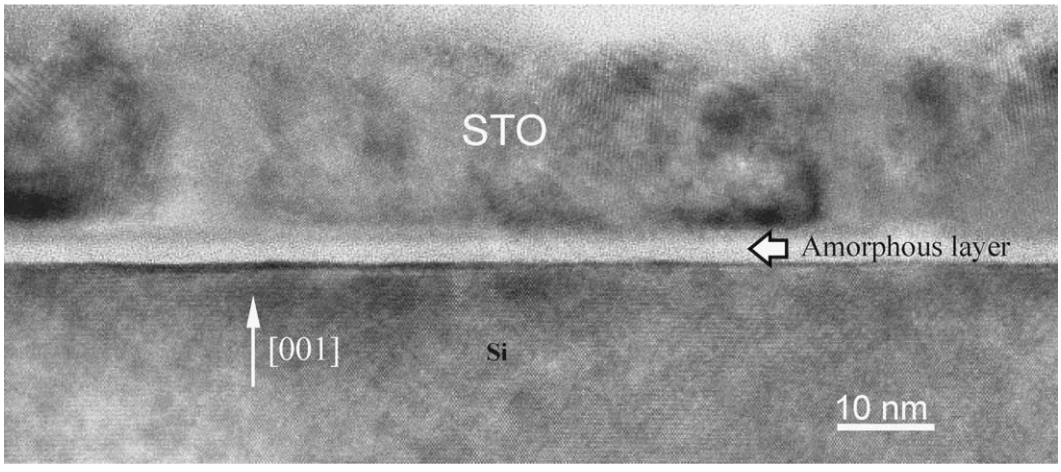

Fig. 4. HRTEM image of the STO/SiO_x/Si interface.

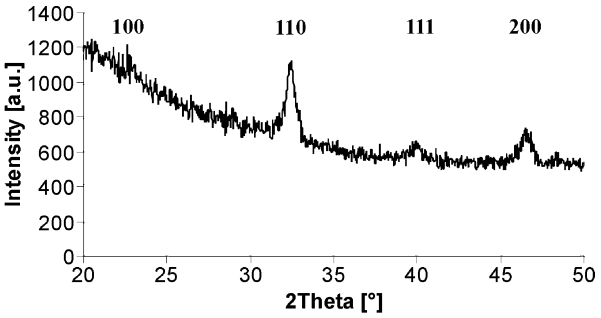

Fig. 5. XRD of a 20 nm STO/SiO_x/Si film in glancing entrance (2°) geometry.

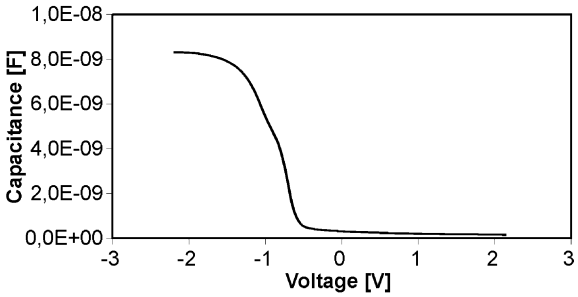

Fig. 6. C–V curve of a typical Pt/STO/SiO_x/*p*-Si/(Ga–In) film stack with 20 nm STO thickness.

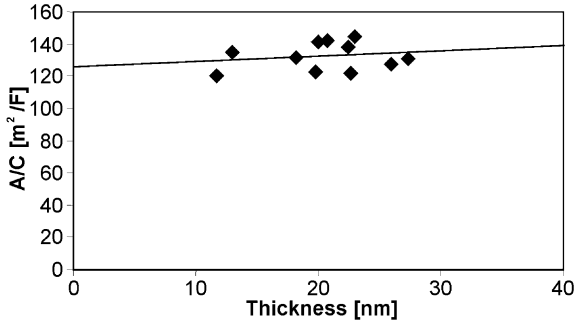

Fig. 7. Reciprocal capacitance for a STO/Si thickness series.

4. Discussion and conclusion

The electrical properties as determined from film thickness series are summarized in Table 2 in terms of the bulk permittivity, ε, and the interfacial capacity, which is expressed by ε_i/t_i. For BST(70/30) we observe a clear indication of a stoichiometry dependence, a decrease of the interfacial capacitance and an increase of the bulk permittivity with increasing Ti content of the films.[4] This tendency cannot be observed for the present STO films, and this observation is independent of the deposition method. This difference indicates that the incorporation of the Ba atoms must be responsible for the changes in the interfacial properties. However, it must be kept in mind, that the values of ε_i/t_i for the STO films are always at the upper limit of the values obtained for BST(70/30). In addition we observe no significant changes with a change of the interface stoichiometry or the growth mode which are possible with the TRIJET® vaporizer. However, this missing effect of the interface stoichiometry is consistent with the independence from the average stoichiometry for the STO layers (Fig. 3b). As these results for the MIM structures were obtained only after annealing of the films after top electrode deposition, different annealing procedures after top electrode deposition have been tested: 650 °C anneals in oxygen or artificial air did not yield higher values. Some tests were accomplished on electrodes with evaporated platinum electrodes. The bulk permittivity was within the error the same but the interface capacity was much reduced. This difference may be related to the surface cleaning property of sputtering.

The physical origin of the dead layer is still under debate and quite different models have been proposed (see e.g. Ref. 7). The observed values of $\varepsilon_i/t_i = 30\ nm^{-1}$ correspond to a permittivity of 3 for a 'subatomic' layer thickness of 0.1 nm, which cannot be detected by analytical methods. On the other hand assuming a significant thickness of the interfacial layer of 1 nm the permittivity would already reach a high-*K* value of 30. Hence, the physical thickness of the low-*K* region must be very thin.

In the last line of Table 2 we show the results of the thickness series on silicon. Within the errors there is no difference between untreated Si(100) and on HF dipped silicon. As only films with thickness in the limited range of 12–27 nm are available the bulk permittivity has a large uncertainty, but it is still within the same range in spite of the much smaller grain size. In contrast to the platinum–STO interface the silicon–STO interface is characterized by an SiO_x layer which is clearly visible in the TEM. This amorphous interlayer had a typical thickness of 2–3nm (Fig. 4). If we accept this value we obtain $\varepsilon_r = 2.7$ for the interfacial layer which somewhat lower than the value of 3.9 expected for perfect SiO_2. Vice versa if we assume a ε_r of 3.9 for SiO_2 we get an interface thickness of 4.3 nm. Although this interfacial layer corroborates the total capacity of the stack it is shown that rather high-*K* STO can be grown on silicon.

Acknowledgements

It is a pleasure to appreciate the help of W. Krumpen in the XRF analysis of the films.

References

1. Kingon, A. I., Maria, J. P. and Streiffer, S. K., Alternative dielectrics to SiO_2 for memory and logic devices. *Nature*, 2000, **406**, 1032–1038.
2. Wilk, G. D., Wallace, R. M. and Anthony, J. M., High-K dielectrics: Current status and materials problems. *J. Appl. Phys.*, 2001, **89**, 5243–5275.

3. Ehrhart, P., Fitsilis, F., Regnery, S., Jia, C.L., Waser, R., Schienle, F., Schumacher, M., Dauelsberg, M., Strzyzewski, P., Juergensen, H., Growth of (Ba,Sr)TiO_3 thin films in a multi-wafer MOCVD reactor. In *Ferroelectric Thin Films IX*, P. C. McIntyre, S. R. Gilbert, Y. Miyasaka, R. W. Schwartz and D. Wouters. MRS Proc., 2001, Vol.655 pp. CC9.4.1–6.
4. Ehrhart, P., Fitsilis, F., Regnery, S., Waser, R., Schienle, F., Schumacher, M., Juergensen, H. and Krumpen, W., Growth of (Ba,Sr)TiO_3 thin films by MOCVD: stoichiometry effects. *Integrated Ferroelectrics*, 2002, **45**, 59–68.
5. Jia, C. L., Urban, K., Hoffmann, S. and Waser, R., Microstructure of columnar-grained $SrTiO_3$ and $BaTiO_3$ thin films prepared by chemical solution deposition. *J. Mater. Res.*, 1998, **13**, 2206–2217.
6. He, J. Q., Regnery, S., Jia, C. L., Qin, Y. L., Fitsilis, F., Ehrhart, P., Waser, R., Urban, K. and Wang, R. H., Interfacial and microstructural properties of $SrTiO_3$ thin films grown by MOCVD on Si(100) substrates. *J. Applied Physics*, 2002, **92**, 7200–7205.
7. Shinamon, L. J., Bowman, R. M. and Gregg, J. M., Investigation of dead-layer thickness in $SrRuO_3/Ba_{0.5}Sr_{0.5}TiO_3$/Au thin film capacitors. *Appl. Phys. Lett.*, 2001, **78**, 1724–1726.